Journal of Thermal Analysis and Calorimetry, Vol. 87 (2007) 1, 247–253

CALORIMETRIC ANALYSES ON AGED Al–4.4Cu–0.5Mg–0.9Si–0.8Mn ALLOY (AA2014 GRADE)

Paola Bassani[1*], *E. Gariboldi*[2] *and G. Vimercati*[2]

[1]National Research Council Institute for Energetics and Interphases, CNR-IENI Unit of Lecco, Corso P. Sposi 29-23900 Lecco, Italy
[2]Politecnico di Milano, Dipartimento di Meccanica, Via La Masa, 34, 20156 Milano, Italy

An Al–4.4Cu–0.5Mg–0.9Si–0.8Mn alloy (IADS 2014 grade) in the solution annealed and peak aged condition was exposed at 170°C for relatively long times (up to about 1800 h) in order to check the stability of the alloy. The investigated aging temperature was in the frame of a research on the long-term mechanical behaviour of such alloy. Microstructure evolution was monitored via calorimetric analyses, metallographic inspections and hardness measurements. Further, X-ray analyses were carried out on selected samples. The attention was focused on differential scanning calorimetry performed at different scanning rates, with the aim of evaluating the kinetics of the precipitation phenomena. Notwithstanding the wide industrial diffusion of this alloy, literature survey showed that there is not a consensus view on the precipitation sequences and on calorimetric peak identification.

The present results show the progressive evolution of calorimetric peaks, corresponding to that of strengthening particles towards more stable phases, proved by the disappearance of exothermic peaks. Activation energy from Kissinger kinetic analysis in the case of aged samples provided scattered values that could be reasonably attributed to an overlapping of transformation peaks. Moreover, in these samples transformations partially occurred before DSC scans, providing non-constant transformation fraction at signal peak temperatures and resulting in different activation energies.

Keywords: *aluminium alloy 2014, DSC, overaging*

Introduction

Aluminium alloys of the 2XXX series are widely used for their good mechanical strength. They are age hardenable alloys, which are serviced in the T6 condition: solution treated and artificially aged at peak hardness.

When these materials are employed at temperatures in the range 130–170°C near to or even corresponding to those of the artificial aging treatment, aging processes proceed, causing material overaging and depleting its mechanical properties such as hardness, tensile strength and toughness. Also long-term high-temperature properties, such as creep behaviour are affected.

It could be of interest to define when the different steps of overaging take place. Simple, rapid tests requiring small amount of material like DSC analyses could be helpful and can be joined to the widely diffused hardness tests which are not able to accurately differentiate the various steps of aging processes.

The precipitation sequence of Al–Cu, Al–Cu–Mg and Al–Cu–Mg–Si alloys has been deeply investigated in the past [1, 2]. Nevertheless, in recent years several researchers still proposed different schemes of precipitation sequences for Al–Cu–Mg–Si alloys [3–6], the presence of which can be related to the relative amount of alloying elements [5, 6]. Further, different designations of precipitates for quaternary Al–Cu–Mg–Si systems can be found in literature.

Focusing the attention on the widely diffused 2014 aluminium alloy (Al–4.4Cu–0.5Mg–0.9Si–0.8Mn alloy) there are three possible precipitation sequences that, according to different authors, can occur during the aging process: (1) $\alpha ss \rightarrow GPZ \rightarrow \vartheta'' \rightarrow \vartheta' \rightarrow \vartheta$ ($CuAl_2$), (2) $\alpha ss \rightarrow GPZ \rightarrow$(GPZII or S'') $\rightarrow S' \rightarrow S$ ($CuMgAl_2$) and (3) $\alpha ss \rightarrow GPZ \rightarrow Q' \rightarrow Q$ ($Cu_2Mg_8Si_6Al_5$ or $Al_3Cu_2Mg_9Si_7$ or $Al_4Cu_2Mg_8Si_7$ [1, 7]).

It is worth reminding the reader that the quaternary phase here referred as Q was alternatively named as λ, W or h-AlCuMgSi by different authors [5].

As a matter of fact, in the quaternary alloys Al–Cu–Si–Mg the actual concurrent precipitation sequences depend on the relative amount of alloying elements. In alloys such as the 2014, the high copper content (about 4 mass%) assures the presence of ϑ precipitation sequence, generally observed for Cu greater than 0.2–0.5 mass%. According to Chakrabarti and Laughlin [5] for high copper quaternary alloys, the precipitation sequence of Mg_2Si (β) phase, in addition to that of θ, could be observed only for

* Author for correspondence: bassani@ieni.cnr.it

1388–6150/$20.00

Akadémiai Kiadó, Budapest, Hungary
Springer, Dordrecht, The Netherlands

Mg/Si ratio greater than 1. For 2014 alloy this condition could be met only for high Mg and low Si in their allowed chemical composition range. Focusing on the more common case for 2014 alloy, with Mg/Si lower than 1, the alternative presence of Q or S precipitation sequences is driven by the amount of Si [5]: very low silicon makes possible the presence of the ternary S phase, while higher amount favours the presence of Q phase and at last of silicon.

The precipitation sequences of age hardenable aluminium alloys are generally investigated by different techniques to optimize the thermal treatment condition. Particular attention has been focused on natural and artificial aging treatments (T4 and T6 condition, respectively) after solution treatment. Less attention was dedicated to lasting overaging phenomena such as those reasonably occurring in the components exposed for long time at relatively high temperatures.

As previously mentioned, calorimetric techniques could provide a relatively simple, fast test on small quantities of material to investigate the sample phases which could be later identified through several more costly and less time-efficient microscopy techniques (OM, SEM, TEM). Once 'calibrated' on the suitable precipitation sequences, the calorimetric analyses of Al alloys could be an efficient tool to evaluate the aging condition of components with relatively small amount of material and effort. Particularly, with respect to other techniques, these analyses are relatively poorly affected by local plastic deformation induced by sampling operations. Small modifications were observed for dislocation density sensitive phenomena, like early stages of precipitation [8], while only extensive plastic deformation can alter calorimetric peaks and even affect later stages of precipitation sequences [9]. On the contrary, hardness measurements are very sensitive to small plastic deformation, which cause scattered data covering up microstructural alteration. Moreover, from isothermal or non-isothermal calorimetric experiments also kinetic features of the transformations, such as the reaction model and Arrhenius parameters, could be obtained. Several methods for analysing the experimental data have been proposed in literature, as outlined in reviews on this matter [10, 11]. Among them, isoconversional methods are known as the most reliable, as they allow for evaluating Arrhenius parameters independently from reaction model [12–14]. Following these ideas, a set of tests at different heating rate in each microstructural condition combined with the Kissinger isoconversional method allows the estimation of activation energies of processes related to calorimetric peaks.

In the present paper the microstructural processes taking place at 170°C in a Al 2014 grade in T6 condition were experimentally investigated by means of DSC techniques and combined results of more conventional methods such as hardness measurements and microstructural (optical microscopy, SEM) examinations.

Experimental

Materials

The alloy used in this investigation is an Al–4.4Cu–0.5Mg–0.9Si–0.8Mn alloy (IADS 2014 grade), the chemical composition of which is given in Table 1.

The alloy was supplied in the form of forged components, solution treated at 505°C, water quenched and aged at 160°C for 16 h. Specimen machined from the component in different sampling orientation were creep tested at 130, 150 and 170°C to investigate its long-term high temperature mechanical behaviour. Creep test results are partially published elsewhere [15]. For the present research study only tests at 170°C were considered, at which overaging phenomena were accelerated and aging times of the order of months allowed examining material in microstructural condition corresponding to years of exposure to lower temperatures. Material of the gripping ends of creep specimens was used to characterize the microstructural modifications that occurred at this temperature. The examination of these regions avoided, in this first step of a wider research programme, any interaction between temperature, stress and creep deformation.

In order to check the material evolution during the heat treatment until T6 condition, samples were machined from the forged component and were solution treated at 505°C for 40 min (W condition) and subsequently aged at 160°C for different times.

Methods

Specimens for metallographic observations and for DSC analyses were cut from bulk samples with a metallographic diamond cutting saw, and grounded to their final shape with emery papers. Final mass of each DSC sample was about 60 mg.

Table 1 Nominal and actual chemical composition of the investigated material

	Mg	Si	Ti	Cr	Mn	Fe	Cu	Al
Actual composition	0.51	0.85	0.00	0.00	1.07	0.22	4.42	bal.
Nominal composition	0.2–0.8	0.5–1.2	<0.15	<0.10	0.4–1.2	<0.70	3.9–5.0	bal.

Tests have been performed with a Setaram Labsys TG-DTA system, equipped with a detector configured for DSC analysis in a temperature range from *rT* up to 800°C. Temperature and heat flow calibration has been carried out using pure indium and zinc melting points. The heating chamber was fluxed with nitrogen. The sample mass was checked before and after DSC runs with a high accuracy balance. No significant increase of the mass was observed. Tests were performed by heating at 5–10–20–30°C min^{-1} from room temperature (*rT*) to 510°C, and then by cooling to *rT* at 30°C min^{-1} in all cases. Scans tests were replicated for the as received (T6) and solubilized (W) conditions.

The material evolution during aging and overaging was monitored by means of 4.91N Vickers Hardness tests performed on a set of sample solution treated and aged at 160°C for different times and on the gripping ends of creep specimens. A selected set of thermally cycled samples or crept specimens were polished with conventional metallographic techniques. After etching with Keller's reagent, they were observed by light optical microscopy and scanning electron microscopy equipped with EDXS (energy dispersion X-ray spectrometry). In order to achieve complementary information, X-ray diffraction tests (using a X-celerator Panalytical with θ–θ configuration and CuK_α radiation) were performed on the solution treated material and on selected aged or crept specimens.

Results

Microstructure characterization

Metallographic observations on specimens in T6 condition and aged at creep test temperatures revealed in all cases the presence of large intermetallic phases, identified as globular Al_2Cu (bright in LOM micrograph in Fig. 1) and blocky shaped and clustered Al–Cu–Mn–Si–Fe particles (dark in Fig. 1), aligned along the longitudinal direction of forged component. Obviously, scanning electron microscopy was not able to resolve the fine non-equilibrium phase responsible for the strength of the alloy in the peak hardness condition. After exposure at relatively high temperature the microstructural features observed with LOM and SEM did not significantly change with respect to those in the as supplied condition.

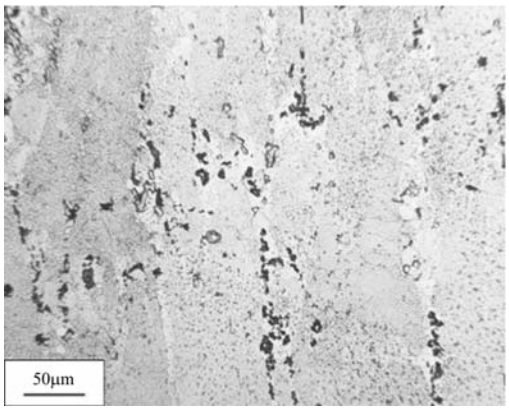

Fig. 1 Typical microstructure of the forged 2014 alloy. (Light optical microscopy)

DSC analyses

The heat flows *vs*. temperature curves during heating of solution treated material are presented in Fig. 2. Five exothermic peaks associated to phase formation/precipitation phenomena and four endothermic peaks, related to dissolution phenomena, were observed. In the low-temperature range (below about 250°C) an exothermic peak (A) at about 100°C was followed by endothermic peak (B), more evident at the higher heating rates. In an intermediate temperature ranges (250–350°C) three exothermic peaks were identified as peaks C, D and E. Between C and D the presence of an endothermic peak (referred as C') could be suggested. The high-temperature range (above 350°C) was characterized by the presence of a broad endothermic peak (F), to which an exothermic peak (G) is superimposed at about 460–470°C. A sharp endothermic peak (H) with typical melting features appears at 520°C. Since melting phenomena are beyond the scope of the present investigation, this peak will not be further taken into account. The peak temperatures of the above identified events for the heat flow heating curve at 20°C min^{-1} are listed in Table 2. Only peaks on which kinetic analysis was carried out are here reported.

The heat flow *vs*. temperature curves at heating rate 20°C min^{-1} of the solution treated, underaged, T6

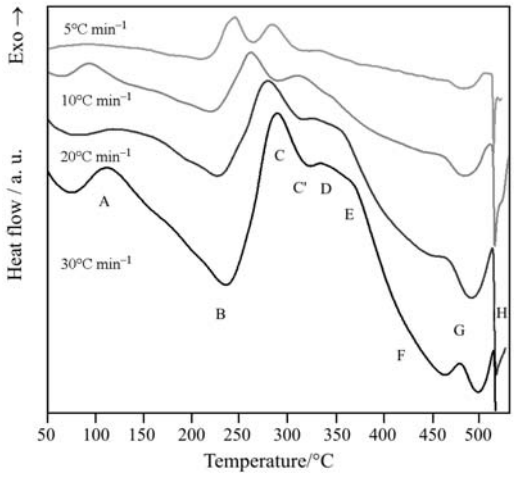

Fig. 2 Heat flow *vs*. temperature curve during heating at different scanning rates of solution treated samples

Table 2 Peak temperature (T_p) of thermal events derived from 20°C heating curves. Values in brackets are not well defined

	T_p/°C								
Peak	Solution treated (W)	W+5 h at 160°C	T6 (16 h at 160°C)	T6+2.9 h at 170°C	T6+24 h at 170°C	T6+72 h at 170°C	T6+143 h at 170°C	T6+273 h at 170°C	T6+1790 h at 170°C
A	110	–	–	–	–	–	–	–	–
B	230	228	–	–	–	–	–	–	–
C	282	261	–	–	–	–	–	–	–
C’	315	280	250	250	255	252	265	273	289
D	332	324	286	283	296	283	307	(312)	–
E	362	349	363	361	360	355	363	364	(356)

and crept materials are shown together for comparison purposes in Fig. 3. Three steps of the aging process can be identified on the basis of the evolution of the peaks with respect to the initial condition. This condition is that of the solution treated sample, where all the peaks previously described are present. In the first step (here in the solution treated and underaged condition) peak A disappears and peaks C, C’ and D shift toward lower temperatures. Moreover C decreases in area whilst C’ increases. A second step can be identified in which peak D progressively disappears (from T6 condition to about additional 200 h spent at 170°C). In the last step also peak E progressively reduces.

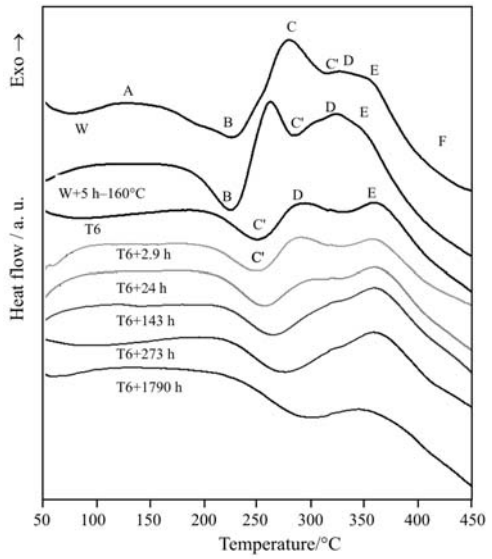

Fig. 3 Heat flow *vs*. temperature curves at heating rate of 20°C min^{-1} of the solution treated (W), underaged (W+3 h at 160°C) as supplied (T6) and overaged conditions

Kinetic analysis from DSC curves

Peaks A, C’, D and E were characterized by means of peak (T_p) temperature (Table 2). An examination of such test results should take into account the fact that smooth and wide peaks can give rise to wide scatter in peak temperatures and enthalpy values and, in any case, values for enthalpy has to be considered as qualitative. For this reason, they were not reported in the present paper.

Kinetic analysis of peaks was brought about by isoconversional Kissinger analysis in order to obtain activation energy of the occurring phenomena [13]. An example of the method used to evaluate activation energy is shown in Fig. 4. The activation energy computed for each specimen condition and peak are listed in Table 3.

Hardness

The hardness evolution of 2014 alloy during artificial aging treatment at 160°C is plotted in Fig. 5a. From an initial value of about 80 HV in the solution treated condition, the material hardness increased in a first

Table 3 Activation energy (E_a) of thermal events taken from 20°C min^{-1} heating curves

	E_a/kJ mol^{-1}								
Peak	Solution treated (W)	W+5 h at 160°C	T6 (16 h at 160°C)	T6+2.9 h at 170°C	T6+24 h at 170°C	T6+72 h at 170°C	T6+143 h at 170°C	T6+273 h at 170°C	T6+1790 h at 170°C
A	55	–	–	–	–	–	–	–	–
B	150	131	–	–	–	–	–	–	–
C	83	111	–	–	–	–	–	–	–
C’	69	120	104	111	112	90	101	105	91
D	83	92	108	123	123	84	79	129	–
E	152	133	125	125	119	112	109	119	117

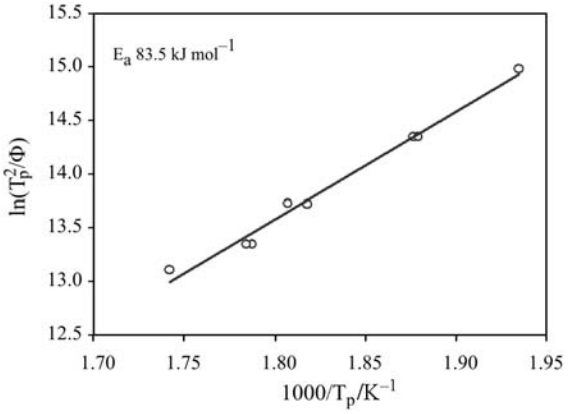

Fig. 4 Kissinger graph for peak C, from solution treated and water quenched samples

stage up to about 100 HV. For times longer than 10 h, hardness further increased to the maximum level of about 155–160 HV. The hardness of the as supplied material (157 HV), nominally aged for 16 h at 160°C, lay within this range. The following exposure at 170°C during creep tests caused overaging phenomena and, correspondingly, a gradual reduction of hardness. After about 1800 h at this temperature it reduced to 118 HV.

In 2014 alloy the overaging processes are presumably related to the lattice diffusion of Cu in Al to form the finely distributed particles of the θ precipitation sequence, which mainly strengthen the alloy matrix. For this reason, the aging times were 'normalized' by multiplying them for the term $e^{-Q/RT}$, defining the normalized time (t_{norm}):

$$t_{norm}=te^{-Q/RT} \quad (4)$$

Plotting hardness *vs*. normalized creep test time from tests at 130, 150 and 170°C, the experimental points of creep specimens were found to align on a single curve [15]. Similarly, in the present paper a normalized time was taken into account to include all the steps of thermal exposure of specimens. In the case of crept specimen, the normalized time include the artificial aging time, the heating step before the beginning of creep test and creep test duration. The hardness data of the material in all the examined conditions are plotted *vs*. the normalized time (t_{norm}) in Fig. 5b. They clearly define an aging curve where the under- and overaged stages can be identified with respect to the peak hardness.

XRD measurements

X-ray pattern in the solution treated specimen is plotted in Fig. 6. From peak position the lattice parameter was derived for the analyzed samples. These values are listed in Table 4. X-ray diffraction highlights the variation of lattice parameter of the alloy during aging. In fact, as expected from literature [16], during aging lattice parameter increased. Even considering the relatively large experimental scatter, a non-monotonic trend with aging time can be observed. This could be related to the presence of different types and quantities of precipitates.

Discussion

Several peaks have been identified using DSC analysis. On the bases of DSC, XRD and hardness test results and of data reported in literature an attempt for identification of the precipitation sequence was made and an explanation of the origin of the main peaks is here proposed. The peaks will be identified under the assumption of concurrent θ and Q precipitation sequences, as suggested in literature [5] on the basis of the actual chemical composition of the forging.

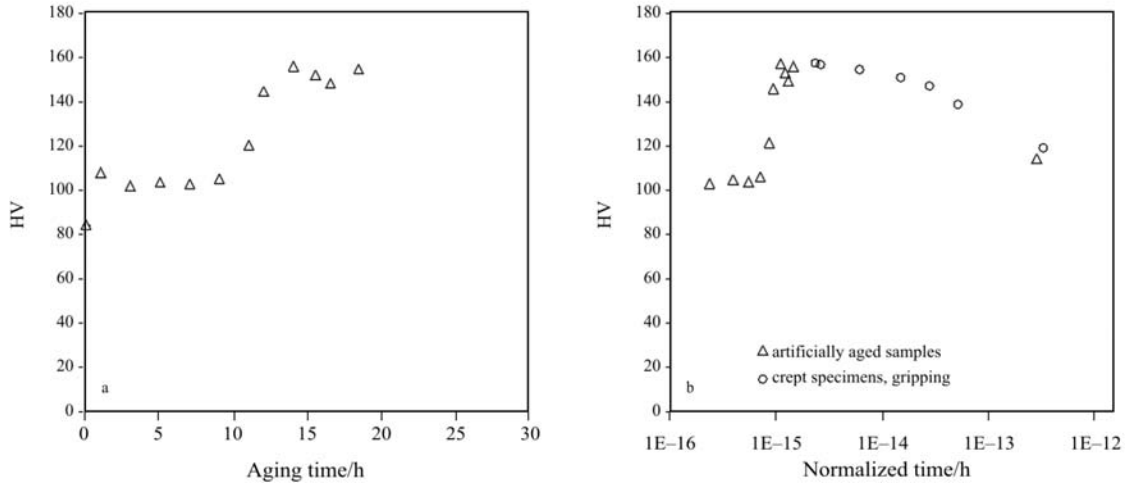

Fig. 5 a – Aging curve at 160°C (after solution treating at 505°C for 40 min and water quenching); b – hardness evolution *vs*. normalized time (t_{norm}) of specimens in different conditions

Table 4 Lattice parameter *a* obtained from XRD of samples in different conditions. In brackets are reported the standard deviation of measurements

	Solution treated (W)	W+3 h at 160°C	T6+16 h at 160°C	T6+2.9 h at 170°C	T6+24 h at 170°C	T6+143 h at 170°C
Lattice parameter/Å (st. dev.)	4.039 (0.002)	4.044 (0.001)	4.051 (0.003)	4.048 (0.001)	4.044 (0.003)	4.048 (0.0009)

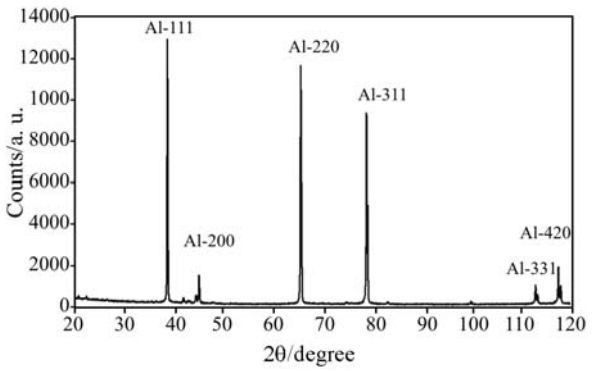

Fig. 6 X-ray pattern of solution treated sample (W)

Peak A

The first thermal effect was identified as formation of GP zones: it was present only in solution treated samples and it was characterized by a T_p of about 100°C, and by activation energy of about 55 kJ mol^{-1}, similar to the activation energy reported in literature for formation of GP zones [17].

Peak B

This second peak, spread over more than 50°C between 170 and 220°C, can be associated to the dissolution of the previously formed GP zones. In fact, peak A can be observed only in the solution treated sample, while B is also observed in the underaged sample, condition in which GP zones are generally present. Also in this case both the temperature range and the activation energy of the event agree with literature data [16].

Peaks C and C'

The evolution of peaks C and C' during aging is more complex. The first peak appears only when the T6 aging condition has not been reached. At intermediate aging temperatures and relatively high copper content this peak hardness condition is associated to the presence of strengthening θ'' phase and to a relatively low amount of θ' [18]. On the basis of the results we can ascribe peak C to θ'' formation. Peak C' could be, on the contrary, associated to θ'' dissolution. This peak could be interpreted to occur at lower temperature during aging until T6 condition is reached and to move toward higher temperatures during overaging. This could be reasonably explained in the following way: the formation of θ" and its subsequent dissolution is favoured when the nucleation of this phase has already started. This happens approximately until T6 condition is reached. During prolonged aging, θ" increases in size and stability; consequently its dissolution is hindered.

Peaks D and E

The following step in the aging process is the formation of θ' and Q'. Following literature [5] θ"could be precursor phase of both these phases, which formation follows θ" dissolution. Peaks D and E could then be ascribed to θ' and Q' formation. As a matter of fact stable θ phase is expected to form at much higher temperature in equilibrium condition (more than 450°C) [18]. Reasonably, also the formation of stable Q phase will be observed at high temperature, then excluding the possibility of ascribing peak E to Q phase formation. Which one of peaks D or E is associated to Q' or θ' should be clarified by TEM investigations, at the moment in progress on the present material.

As aging proceeds during exposure of the as forged material at intermediate temperatures during creep tests, the formation of Q' and/or θ' proceeds. Consequently, the respective exothermal peaks progressively decrease and finally disappear.

In the case of crept samples, the activation energy from Kissinger kinetic analysis provided rather scattered values, particularly for peak D. There are two main reasons for this scatter: the first is the superimposition of peaks would require deconvolution of each contribution for correct evaluation of peak temperature. Moreover for these samples transformation are partially occurred during creep test, i.e. before DSC scans, providing non-constant transformation fraction at signal peak temperatures, resulting in different activation energy.

Conclusions

The examination of Al-2014 alloy exposed at 170°C for up to 1800 h after solution annealed and peak aging allowed examining the material in several steps of its aging process and DSC analyses were confirmed to

be a useful tool for monitoring the evolution of the occurring processes. The DSC analysis gave in the present case the opportunity to evaluate the degree of overaging, not satisfactorily described by hardness evolution.

The present results show the progressive evolution of calorimetric peaks, corresponding to that of hardening particles towards more stable phases. The suggested identification of calorimetric peaks of crept samples was made through literature survey on the same alloy: A-GPZ formation, B dissolution of GPZ, C and C' formation and dissolution of θ", respectively, D and E formation of θ'and Q'. As far as these two latter peaks are concerned, the attribution of each peak to the correct phase on the basis of the presently available results seems venturous and further investigations are needed to clarify these peaks. In any case, both peaks are well defined and this suggests that the amount of the Q' is not negligible with respect to θ'. It can be stated that, for aging time greater than 140 h at 170°C the presence of Q'+θ' prevails on that of θ".

The use of temperature-normalized time allows, within suitable temperature range, to merge different aging periods at different temperatures.

References

1 J. E. Hatch, Ed., American Society for Metals, Metals Park, OH, USA 1984.
2 R. D. Doherthy, Physical Metallurgy, R. W. Cahn, P. Haasen, Eds, Elsevier Science BV, Amsterdam 1996, pp. 1363, 1505.
3 S. Abis, M. Massazza, P. Menegucci and G. Riontino, Scripta Materialia, 45 (2001) 685.
4 C. Badini, F. Marino and E. Vernè, Mater. Sci. Eng. A, A191 (1995) 185.
5 D. J. Chakrabarti and D. E. Laughlin, Progr. Mater. Sci., 49 (2004) 389.
6 W. F. Miao and D. E. Laughlin, Metal. Mater. Trans., A, 31 (2000) 361.
7 C. Wolverton, Acta Mater., 49 (2001) 3129.
8 G. Angella, P. Bassani, A. Tuissi, D. Ripamonti and M. Vedani, Mater. Sci. Forum, 503–504 (2006) 493.
9 M. J. Starink, A. J. Hobson and P. J. Gregson, Scripta Materialia, 34 (1996) 1711.
10 G. Biroli, G. Caglioti, L. Martini and G. Riontino, Scripta Materialia, 39 (1998) 197.
11 H. Tanaka, Thermochim. Acta, 267 (1995) 29.
12 T. Ozawa, Thermochim. Acta, 355 (2000) 35.
13 M. J. Starink, Thermochim. Acta, 404 (2003) 163.
14 S. Vyazovkin, Thermochim. Acta, 355 (2000) 155.
15 E. Gariboldi and F. Casaro, Mater. Sci. Eng. A, DOI: 10.1016/j.msea.2006.04.153.
16 I. Wierszyllovski, S. Wieczorek, A. Stankowiak and J. Samolczyk, JPEDAV, 26 (2005) 555.
17 G. Riontino, S. Abis and P. Mengucci, Mater. Sci. Forum, 331–337 (2000) 1055.
18 R. E. Smallman and R. J. Bishop, Modern Physical Metallurgy and Materials Engineering-Science, Process, Application, 6th Edition, Butterworth–Heinmann, 1999.

DOI: 10.1007/s10973-006-7836-3